AJNR

White Matter Alteration of the Cingulum in Parkinson Disease with and without Dementia: Evaluation by Diffusion Tensor Tract–Specific Analysis

K. Kamagata, Y. Motoi, O. Abe, K. Shimoji, M. Hori, A. Nakanishi, T. Sano, R. Kuwatsuru, S. Aoki and N. Hattori

AJNR Am J Neuroradiol 2012, 33 (5) 890-895
doi: https://doi.org/10.3174/ajnr.A2860
http://www.ajnr.org/content/33/5/890

ORIGINAL RESEARCH

White Matter Alteration of the Cingulum in Parkinson Disease with and without Dementia: Evaluation by Diffusion Tensor Tract–Specific Analysis

K. Kamagata
Y. Motoi
O. Abe
K. Shimoji
M. Hori
A. Nakanishi
T. Sano
R. Kuwatsuru
S. Aoki
N. Hattori

BACKGROUND AND PURPOSE: In PD, the neurodegenerative process begins in the brain stem and extends to the limbic system and finally into the cerebral cortex. We used diffusion tensor tractography to investigate the FA of the cingulate fiber tracts in patients with PD with and without dementia.

MATERIALS AND METHODS: Fifteen patients with PD, 15 patients with PDD, and 15 age-matched healthy controls underwent diffusion tensor imaging with a 3T MR imager. Diffusion tensor tractography images of the anterior and posterior cingulate fiber tracts were generated. Mean diffusivity and FA were measured along the tractography of the anterior and posterior cingulate fiber tracts. One-way ANOVA with the Scheffé post hoc test was used to compare results among the groups.

RESULTS: FA was significantly lower in patients with PDD than in healthy controls in both the anterior and the posterior cingulate fiber tracts ($P = .003$, $P = .015$) and significantly lower in patients with PD than in healthy controls ($P = .003$) in the anterior cingulate fiber tract. There were no significant mean diffusivity differences among the groups. MMSE and FA values of the anterior cingulate fiber tracts in patients with PDD were significantly correlated ($r = 0.633$, $P < .05$).

CONCLUSIONS: The reduced FA in patients with PD and PDD might reflect neuropathologic changes such as Lewy body pathology in the cingulate fibers. This abnormality might contribute to the dementing process in PD.

ABBREVIATIONS: CFT = cingulate fiber tract; FA = fractional anisotropy; HSD = Honestly Significant Difference; MD = mean diffusivity; MMSE = Mini-Mental State Examination; PD = Parkinson disease; PDD = Parkinson disease with dementia; UPDRS = Unified Parkinson's Disease Rating Scale

PD is the second most frequent neurodegenerative disorder after Alzheimer disease.[1] It is clinically characterized by a complex motor disorder known as parkinsonism, which is manifested principally by resting tremor, slowness of initial movement, rigidity, and general postural instability.[2] In PD, the primary pathologic changes involve loss of nigrostriatal dopaminergic neurons and the presence of Lewy bodies (α-synuclein–immunoreactive inclusions), with neuronal loss in numerous brain regions.[3] The presence of these Lewy body aggregations, which result, in part, from protein misfolding, is mandatory for neuropathologic confirmation of the clinical diagnosis. The neurodegenerative process (Lewy body pathology) begins in the brain stem and extends into the limbic system and finally into the cerebral cortex.[3-6] Extension of the neurodegenerative process beyond the brain stem is probably the basis for some of the clinical features, including nonmotor deficits such as dementia. Although dementia frequently occurs in the late stages of PD and is associated with increasing disability, mainly in elderly cohorts,[7,8] its neuroanatomic basis is still controversial. In particular, it is unclear whether cognitive deterioration is primarily a cortical or a subcortical process.

To distinguish these pathophysiologic changes in PD, conventional MR imaging has so far been unsuccessful. A noninvasive technology such as diffusion tensor imaging would be helpful for understanding changes at the microstructural level, as well as for monitoring disease progression and improving prognosis in terms of these aspects of PD. A recent study including only patients with newly diagnosed PD used high-resolution diffusion tensor imaging at 3T to evaluate rostral, middle, and caudal ROIs within the substantia nigra on a single section of the midbrain. This study found that patients with PD could be completely distinguished from the control group on the basis of reduced FA values in the caudal ROI of the substantia nigra.[9] In another study, diffusion tensor imaging and ROI analyses revealed changes in FA in the cingulum in patients with PD without dementia relative to controls.[10] Changes in FA have also been found in the frontal lobes, including the supplementary motor area, the presupplementary motor area, and the cingulum, in patients with PD without dementia relative to controls by using statistical parametric mapping analysis in conjunction with diffusion tensor imaging.[11] In a diffusion tensor imaging study of subjects with PDD ($n = 11$), Matsui et al[12] reported a reduction in the FA in the posterior cingulate compared with the FA in subjects with PD ($n = 26$) and healthy controls ($n = 10$). These findings support the notion that the posterior cingulate may play an im-

Received June 6, 2011; accepted after revision August 4.

From the Departments of Radiology (K.K., K.S., M.H., A.N., R.K., S.A.) and Neurology (Y.M., T.S., N.H.), Juntendo University School of Medicine, Tokyo, Japan; and Department of Radiology (O.A.), Nihon University School of Medicine, Tokyo, Japan.

Koji Kamagata and Yumiko Motoi contributed equally to this study.

Please address correspondence to Koji Kamagata, MD, Department of Radiology, Juntendo University School of Medicine, 2-1-1, Hongo Bunkyo-ku Tokyo 113-8421 Japan; e-mail: kkamagat@juntendo.ac.jp

http://dx.doi.org/10.3174/ajnr.A2860

Table 1: Demographic characteristics of subjects

	Control ($n = 15$)	PD ($n = 15$)	PDD ($n = 15$)	*P* Value (Control vs PD)	*P* Value (Control vs PDD)	*P* Value (PD vs PDD)
Sex, male/female	6:9	9:6	8:7	NS	NS	NS
Age in years, (mean) (SD)	69.5 (6.9)	69.8 (5.9)	71.3 (5.6)	NS	NS	NS
Disease duration in months (mean) (SD)	NA	70.6 (58)	139.0 (96.5)	NA	NA	<.05
Hoehn and Yahr stage (SD)	0	2.3 (1.3)	3.0 (0.7)	NA	NA	<.05
MMSE (SD)	28.5	26.1 (3.2)	20.2 (4.0)	NS	<.01	<.01
UPDRS-III score (SD)	NA	19.0 (12.0)	27.1 (9.9)	NA	NA	<.05
Levodopa dosage (mg/day) (median) (SD)	0	409.1 (280.3)	687.0 (126.0)	NA	NA	<.05

Note:—NA indicates not applicable; NS, not significant ($P > .05$).

portant role in the pathologic process of PDD. On pathologic examination, Kövari et al[13] reported that there was a highly significant correlation between the clinical dementia rating scores and regional Lewy body densities in the entorhinal cortex and anterior cingulate gyrus.

The posterior cingulum is an important part of the Papez circuit, which is important for the processing of episodic memory. Posterior CFTs connect the anterior thalamus, cortical cingulum, association cortices, and hippocampus.[14] The importance of the cingulum goes far beyond episodic memory. As previously suggested, the perigenual anterior cingulate cortex is involved in affect; the subgenual subregion of the anterior cingulate cortex, in visceromotor control; the middle cingulate cortex, in response selection (including the dorsal middle cingulate cortex in skeletomotor control); the posterior cingulate cortex, in visuospatial processing; and the retrosplenial cingulate cortex, in memory access.[15]

The cause of dementia in PD is still under debate, but we consider that 1 underlying cause of dementia might be the process of neurodegeneration in the anterior and posterior cingulate gyrus over the brain stem, given the general role of the cingulate gyrus and the pathology of PD as described thus far.

We hypothesized that patients with PD with and without dementia show diffusion abnormalities in the cingulate fibers and that these diffusion abnormalities are an important part of the pathologic process of PD.

Almost all studies of diffusion tensor imaging in PD have used either ROI diffusion tensor imaging[10,12] or statistical parametric mapping methods.[11] Diffusion tensor tractography is one of the most promising imaging processing techniques because it enables both visualization of the fiber pathways in the brain and quantitative analysis of specific fiber bundles.[16,17]

We, therefore, compared diffusion abnormalities in the cingulate fibers in patients with PD with and without dementia and healthy controls by using diffusion tensor tractography.

Materials and Methods

Subjects

This study was approved by an institutional review board, and informed consent was obtained from all participants before evaluation. For subjects who, because of cognitive impairment, were determined by the clinician not to have the capacity to give consent, a legally authorized surrogate provided consent. The demographic characteristics of the subjects are shown in Table 1. In all patients with PD, the disease had been diagnosed by neurologists and fulfilled the UK Parkinson's Disease Society Brain Bank criteria.[18] PD was staged according to the Hoehn and Yahr scale, and the subjects underwent the Japanese version of the MMSE to assess cognitive dysfunction.[19] PDD was diagnosed in accordance with recently published guidelines,[20] and patients with probable PDD were selected. All patients with PD and PDD were taking levodopa at the time of the MR imaging and clinical examination. Eighteen months or more after scanning, all patients remained free of atypical parkinsonism and continued responding satisfactorily to antiparkinsonian therapy. Fifteen healthy subjects were recruited from the general population as control subjects, and they were carefully matched in age to the patients. Individuals with any history of hypertension, diabetes mellitus, cardiovascular disease, stroke, brain tumor, epilepsy, PD, dementia, depression, drug abuse, or head trauma were excluded as controls.

MR Imaging

The brains of all patients were examined with a 3T MR imaging unit (Achieva; Philips Healthcare, Best, the Netherlands) and an 8-channel-array receiving head coil for sensitivity encoding parallel imaging. Regular structural images such as T1-weighted spin-echo images, T2-weighted turbo-spin-echo images, and fluid-attenuated inversion recovery images were obtained before acquisition of diffusion tensor images. Diffusion tensor imaging was performed by using the spin-echo echo-planar technique (TR/TE, 5443/70 ms; matrix size, 128 × 128; FOV, 224 × 224 mm^2; section thickness, 3 mm with no gap). Images were obtained with both 32-direction diffusion encoding ($b = 1000$ s/mm^2 for each direction) and no diffusion encoding ($b = 0$ s/mm^2). A total of 50 axial section images were obtained, covering the whole cerebrum. Scanning time was 7 minutes 17 seconds.

Diffusion Tensor Data Postprocessing

Diffusion tensor imaging data were transferred to an off-line workstation. Maps of FA and MD were computed by using dTV II and Volume-One 1.72 (http://www.volume-one.org), developed by Masutani et al (University of Tokyo; diffusion tensor visualizer available at http://www.ut-radiology.umin.jp/people/masutani/dTV.htm).[17,21] Diffusion tensors were computed, and fiber tracts were created by using interpolation along the z-axis to obtain data (voxel size, 2.0 × 2.0 × 3.0 mm^3). Using 33 sets of images (32 sets of images with $b = 1000$ s/mm^2, 1 set of images with $b = 0$ s/mm^2), we created color-coded maps. On the color maps, red was assigned to left-right, green to the anteroposterior, and blue to the craniocaudal direction.[22] Fiber tracts were based on the fiber assignment made by using the continuous tracking approach[23] to obtain a 3D tract reconstruction. Identification of fiber tracts was initiated by placing a "seed" and a "target" area in anatomic regions through which the particular fibers

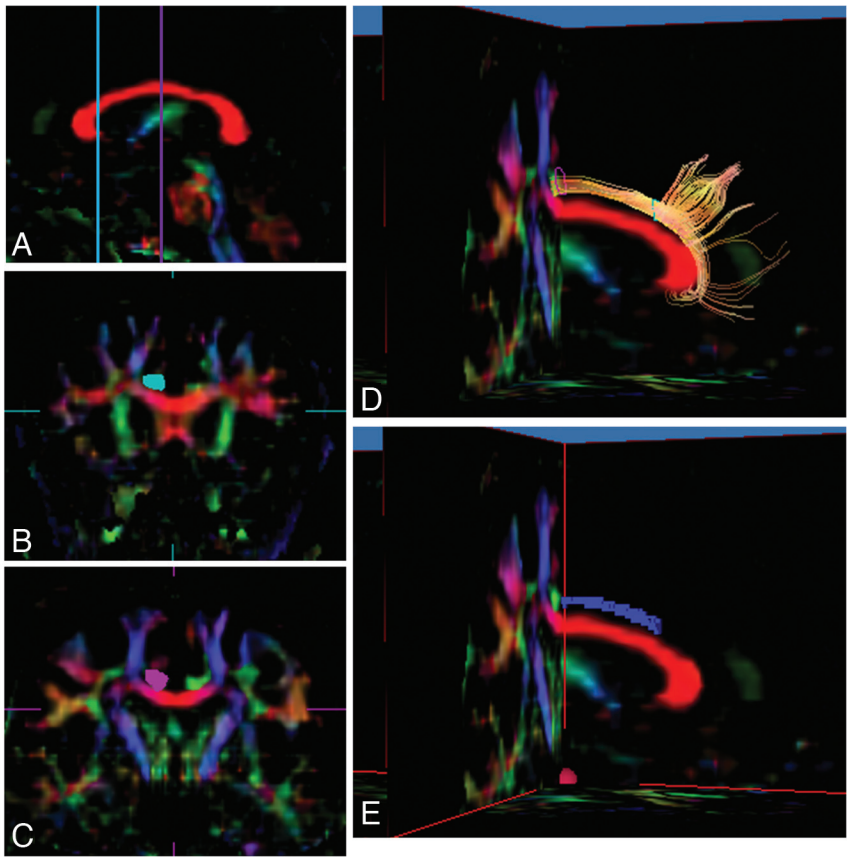

Fig 1. Diffusion tensor tractography images of the right cingulate, fiber tracts (CFTs), and voxelization along with diffusion tensor tractography images of the anterior CFTs. *A*, Sagittal section of the color-coded map was used to determine coronal sections at the level of the genu of the corpus callosum and the middle of the corpus callosum. *B*, The seed ROI, including the entirety of the CFTs (*light blue area*), was placed manually on a coronal section of the color maps at the level of the genu of the corpus callosum. *C*, The target ROI, including the entirety of the CFTs (*purple area*), was placed manually on a coronal section of the color maps at the level of the center of the corpus callosum in the sagittal plane. *D*, Tractographic image of the right anterior CFTs was generated from the seed ROI (light blue line) to the target region of interest (purple line). *E*, In this study, the anterior CFTs were defined as the CFTs between the seed ROI and the target ROI. Voxelization was performed along the right anterior CFTs between the seed ROI and the target ROI (blue voxels), and FA values in coregistered voxels were calculated.

were expected to course.[24] We performed diffusion tensor tractography of the anterior and posterior CFTs and also the corticospinal tracts as a control procedure. The FA threshold for tracking was set at 0.18, and the stop length was set at 160 steps, in accordance with a previous report by Yasmin et al.[25] Tract measurements were performed by 2 of the authors (K.S., K.K.), who were blinded to the disease status of the subjects.

Tractography of the anterior CFT was performed from the seed ROI in the anterior part of the CFT to the target ROI in the middle of the CFT, and tractography of the posterior CFT was performed from the seed ROI in the posterior part of the CFT to the target ROI in the middle of the CFT. Color maps were created to enable the exact and objective placement of these ROIs in the CFTs. Coronal sections at the level of the genu of the corpus callosum and the center of the corpus callosum were identified on a sagittal section of the color map (Fig 1*A*). The CFTs were shown as green in the coronal sections. The seed and target ROIs of the anterior CFTs were drawn manually. The seed region of interest included the entirety of the green part indicating the CFT on a coronal section of the color map at the level of the genu of the corpus callosum, with the green being replaced with light blue to mark the ROI (Fig 1*B*). The target ROI included the entirety of the green part on a coronal section of the color maps at the level of the center of the corpus callosum, with the green replaced by purple to mark the ROI (Fig 1*C*). A tractographic image of the anterior CFT was then generated (Fig 1*D*).

For the posterior CFTs, coronal sections at the level of the splenium of the corpus callosum and the center of the corpus callosum were identified on a sagittal section of the color map (Fig 2*A*). The seed and target ROIs of posterior CFTs were also drawn manually, including the entirety of the green part on a coronal section of the color maps at the level of the splenium of the corpus callosum for the seed (Fig 2*B*) and the center of the corpus callosum for the target (Fig 2*C*). A tractographic image of the posterior CFTs was then generated (Fig 2*D*). The trackline voxelization function of the dTV II software voxelizes the tracking line of the white matter tract by using the original tensor parameters. In this study, anterior and posterior CFTs were defined as the CFTs between the seed ROI and the target ROI. The anterior and posterior CFTs were voxelized between the seed ROI and the target region of interest (Figs 1*E* and 2*E*), and MD and FA values in coregistered voxels were calculated.

Tractography of the corticospinal tract was performed by placing the seed ROI on the cerebral peduncle and the target ROI on the superior precentral gyrus and adjacent white matter, in accordance with a previous report by Yasmin et al.[25] A tractographic image of the corticospinal tract was then generated. The corticospinal tract between the seed region of interest and the target region of interest was voxelized, and MD and FA values in coregistered voxels were calculated.

Statistical Analysis

Statistical analysis of demographic and clinical data was ANOVA with the Tukey HSD test for continuous variables and a χ^2 test for categoric data. The criterion of statistical significance was $P < .05$.

Statistical analyses were performed by using Statistical Package for the Social Sciences for Windows, Release 8.0 (SPSS, Chicago, Illinois). One-way ANOVA was used to compare the averaged MD and FA among patients with PD or PDD and healthy controls. The Scheffé correction was used for post hoc analysis. A Bonferroni correction was applied for the number of comparisons ($n = 3$: [anterior cingulum, posterior cingulum, corticospinal tract], setting the level of significance at $P < .05/3 = .016$). The Spearman rank-order correlation

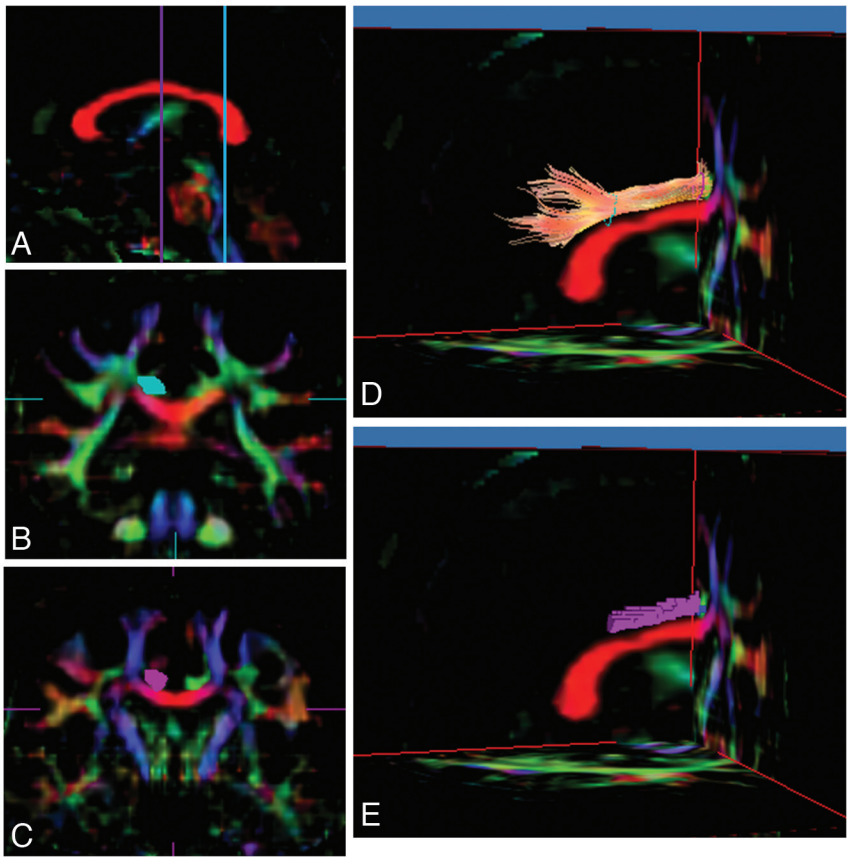

Fig 2. Diffusion tensor tractography images of the right cingulate. Fiber tracts (CFTs) and voxelization along with diffusion tensor tractography of the posterior CFTs. *A*, Sagittal section of the color-coded map was used to determine coronal sections at the level of the splenium of the corpus callosum and the middle of the corpus callosum. *B*, The seed ROI, including the entirety of the CFTs (light blue area), was placed manually on a coronal section of the color maps at the level of the splenium of the corpus callosum. *C*, The target region of interest, including the entirety of the CFTs (purple area), was placed manually on a coronal section of the color maps at the level of the center of the corpus callosum in the sagittal plane. *D*, A tractographic image of the right posterior CFTs was generated from the seed ROI (light blue line) to the target ROI (purple line). *E*, In this study, the posterior CFTs were defined as the CFTs between the seed ROI and the target ROI. Voxelization was performed along the right posterior CFTs between the seed ROI and the target ROI (purple voxels), and FA values in coregistered voxels were calculated.

test was used to investigate the correlations between the imaging measurements and continuous clinical variables.

Results

The 3 groups did not differ by age ($P > .53$, ANOVA) or sex distribution ($P > .68$, χ^2) (Table 1). As expected, patients with PDD scored significantly lower than patients with PD and control subjects on the MMSE ($P < .01$, $P < .01$, ANOVA with the Tukey HSD test), but patients with PD and control subjects did not differ significantly on the MMSE. There were significant differences in disease duration, Hoehn and Yahr stage, UPDRS-III score, and levodopa dosage (milligrams/day) between patients with PD and those with PDD (Table 1).

Reproducibility was determined on the basis of fiber counts and expressed as an intraclass correlation coefficient; the coefficient was 0.96 for the anterior CFTs, 0.94 for the posterior CFTs, and 0.96 for the corticospinal tracts. No significant differences were seen in either MD or FA between the right and left anterior or posterior CFTs ($P > .05$). Averaged values were, therefore, used for further statistical analyses.

There was a significant correlation between the MMSE score and FA value in the anterior CFTs ($r = 0.633$, $P < .05$) in patients with PDD (Fig 3). Measured FA and MD values of the anterior and posterior CFTs were not significantly correlated with disease duration or Hoehn and Yahr stage ($P > .05$) in patients with either PD or PDD.

FA measured in the anterior CFTs was significantly lower in patients with PD and PDD than in healthy controls ($P = .003$, $P = .003$) (Table 2). FA measured in the posterior CFTs was significantly lower in patients with PDD than in healthy controls ($P = .002$). There were no significant diffusion differences in the corticospinal tracts among the groups (Table 2).

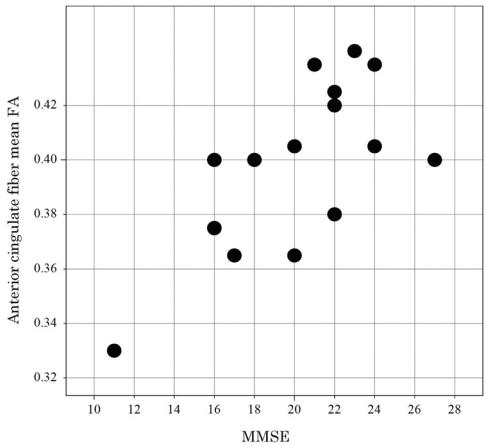

Fig 3. FA values in the anterior cingulate fiber tracts in patients with PDD were significantly correlated with the MMSE scores ($r = 0.633$, $P < .05$).

Discussion

We compared diffusion tensor imaging measurements of the cingulate fasciculi in patients with PD and PDD with those in healthy controls by using diffusion tensor tract-specific analyses. Our major findings were that the measured mean FA in the anterior CFTs was significantly lower in patients with PD and PDD than in healthy controls and that the measured mean FA in the posterior CFTs was significantly lower in patients with PDD than in healthy controls. Most interesting, there was

Table 2: Comparison of MD and FA in patients and control subjects[a]						
	HC	PD	PDD	HC > PD	HC > PDD	PD > PDD
Anterior CFTs						
FA	0.441 ± 0.035[a]	0.399 ± 0.028	0.399 ± 0.031	$P = .003$[b]	$P = .003$[b]	$P = .90$
MD[c]	0.758 ± 0.025	0.789 ± 0.034	0.775 ± 0.031	$P = .031$	$P = .33$	$P = .47$
Posterior CFTs						
FA	0.519 ± 0.038	0.489 ± 0.040	0.477 ± 0.040	$P = .09$	$P = .015$[b]	$P = .72$
MD	0.755 ± 0.046	0.759 ± 0.022	0.770 ± 0.027	$P = .94$	$P = .32$	$P = .51$
Corticospinal tract						
FA	0.655 ± 0.020	0.651 ± 0.022	0.651 ± 0.024	$P = .89$	$P = .87$	$P = .99$
MD[c]	0.751 ± 0.026	0.775 ± 0.025	0.756 ± 0.031	$P = .077$	$P = .92$	$P = .17$

Note:—HC indicates healthy controls.
[a] Values are mean ± SD.
[b] Indicates statistical significance ($P < .016$).
[c] Mean diffusivity values are expressed as 10^{-3} mm^2/s.

also a significant correlation between MMSE scores and FA values of the anterior CFTs in patients with PDD.

Diffusion tensor imaging is capable of measuring the characteristics of local microstructural water diffusion in brain tissue. One representative diffusion tensor measurement is FA, which describes the degree of water molecule anisotropy or the directional preference of the water diffusion process. FA abnormalities in the brain are interpreted pathologically as being caused by loss of neurons or glia or by gliosis or demyelination.[26]

The existing literature already includes results showing diffusion abnormalities in the cingulum bundle.[10-12,27] However, there has been no report to date of the use of tractography to show diffusion abnormalities in the cingulum bundle in patients with PD and PDD. Diffusion tensor tractography enabled us to clearly identify the anterior CFTs and posterior CFTs and measure diffusion parameters more precisely than with a manually drawn ROI study. Use of diffusion tensor tractography avoided contamination of data by anterior and posterior CFTs from adjacent components such as CSF or callosal fibers. Taoka et al[28] compared a tract-specific method and an ROI method for evaluating the diffusion parameters of 3 cerebellar peduncles in subtypes of spinocerebellar degenerative disease. They found that the tract-specific method tended to show significant differences more clearly than the ROI method because instabilities in the placement of ROIs in anatomic structures directly result in instability of the values measured with the ROI method.[28] We consider the results of the tractography to be more reproducible and more accurate than those of other research in the existing literature.

The decreased FA in the anterior CFTs in patients with PD and PDD may be associated with the pathologic process of PD. Brains of patients with PD have Lewy bodies in various areas, including the cingulate cortex.[3-6] Neuropathologically, postmortem material from patients with PD is divided into 6 subgroups (stages 1–6) that differ from each other by virtue of changes in the topographic distribution pattern and severity of Lewy body involvement.[4-6] Postmortem material from patients with PD who manifest clinical findings consistent with sporadic PD can be assigned to 1 of 3 subgroups (stages 4–6). Because Lewy bodies appear in the anterior cingulate gyrus in stage 5,[3-6] neurodegeneration may occur in the anterior CFTs adjacent to the anterior cingulate gyrus.

The FA values of the anterior CFTs were significantly correlated with the MMSE scores. This result is in good agreement with that of a previous pathologic study in which Kövari et al[13] reported a highly significant correlation between the clinical dementia rating scores and regional Lewy body densities in the anterior cingulate gyrus.

The decreased FA values in the posterior CFTs of patients with PDD may be related to the pathologic processes responsible for dementia in PD. Atrophy in the limbic and paralimbic regions occurs in patients with PD without dementia, though less markedly so than in patients with PDD.[29,30] Metabolic abnormalities in the posterior cingulate regions[31,32] and cerebral blood flow reduction in the anterior cingulate cortex[33,34] have been reported in patients with PDD. A reduction in cerebral blood flow in the posterior cingulate cortex has also been reported in PDD.[33] In several previous studies of neuropsychologic diseases such as amyotrophic lateral sclerosis, posttraumatic stress disorder, and schizophrenia, metabolic and cerebral blood flow abnormalities in the cortex and diffusion abnormalities in the white matter tracts that connect the affected regions of the cortex have been reported.[16,35,36]

Our definition of the posterior cingulum bundle probably corresponds to the white matter directly below the posterior cingulate cortex and dorsal middle cingulate cortex, as described by Vogt et al.[15] They have also reported on the relationship between the posterior cingulate cortex and visuospatial perception. There have been reports of a general reduction in visuospatial perception in patients with PDD.[37,38] Diffusion impairment in the posterior cingulum bundle may reflect the particular pathophysiology of PDD.

The pathologic processes responsible for dementia in patients with PD are still controversial. Cortical Lewy bodies; striatal and extrastriatal dopamine deficiencies; loss of ascending noradrenergic, cholinergic, and serotonergic projections to the cortex; disruption of corticostriatal connections; coexistence of Alzheimer disease pathology; and frontal dysfunction have all been considered responsible for dementia in PD.[39-41] Although the pathologic processes responsible for dementia in PD may be multifaceted, our results show that the posterior CFT is important in the dementing process in PDD.

Some limitations of our study need to be addressed. First, because the diagnoses of PD and PDD were not histopathologically confirmed, the possibility of misdiagnosis remains. However, the validity of the diagnoses is supported by the fact that 18 months or more after being scanned, all the patients remained free of atypical parkinsonisms and continued to respond satisfactorily to antiparkinsonian therapy. Second, the

small size of our samples may have limited the detection of group differences, especially in the comparison of neuropsychological profiles and FA values. Third, the seed and target ROIs were drawn manually, and the reproducibility of the measurements was uncertain. However, rater bias was prevented by blinding, all ROIs were drawn by 2 of the authors, and the intraclass correlation coefficients were 0.94–0.96.

Conclusions

The decreased FA found in patients with PD on tract-specific analysis is likely due to neuronal loss, gliosis, or demyelination in the white matter of the cingulum. Our results suggest that these reduced values reflect neuropathologic changes—such as Lewy body pathology in the cingulate gyrus—that may play important roles in the dementing process in PD.

Acknowledgments

We thank Nozomi Hamasaki and Syuji Sato, MR imaging technologists, for their skillful performance in data acquisition; Toshino Suzuki, Tomomi Okamura, Yasmin Hasina, as research assistants; Yuriko Suzuki and Masaru Takashima, Philips Healthcare, for their technical assistance. We also thank Keisuke Sasai for administrative assistance.

References

1. de Lau LM, Breteler MM. **Epidemiology of Parkinson's disease.** *Lancet Neurol* 2006;5:525–35
2. Obeso JA, Rodriguez-Oroz MC, Rodriguez M, et al. **Pathophysiology of the basal ganglia in Parkinson's disease.** *Trends Neurosci* 2000;23:S8–19
3. Braak H, Del Tredici K. **Invited article: nervous system pathology in sporadic Parkinson disease.** *Neurology* 2008;70:1916–25
4. Braak H, Del Tredici K, Bratzke H, et al. **Staging of the intracerebral inclusion body pathology associated with idiopathic Parkinson's disease (preclinical and clinical stages).** *J Neurol* 2002;249(suppl 3):III/1–5
5. Braak H, Del Tredici K, Rub U, et al. **Staging of brain pathology related to sporadic Parkinson's disease.** *Neurobiol Aging* 2003;24:197–211
6. Braak H, Ghebremedhin E, Rub U, et al. **Stages in the development of Parkinson's disease-related pathology.** *Cell Tissue Res* 2004;318:121–34
7. Aarsland D, Tandberg E, Larsen JP, et al. **Frequency of dementia in Parkinson disease.** *Arch Neurol* 1996;53:538–42
8. Marder K, Tang MX, Cote L, et al. **The frequency and associated risk factors for dementia in patients with Parkinson's disease.** *Arch Neurol* 1995;52:695–701
9. Vaillancourt DE, Spraker MB, Prodoehl J, et al. **High-resolution diffusion tensor imaging in the substantia nigra of de novo Parkinson disease.** *Neurology* 2009;72:1378–84
10. Gattellaro G, Minati L, Grisoli M, et al. **White matter involvement in idiopathic Parkinson disease: a diffusion tensor imaging study.** *AJNR Am J Neuroradiol* 2009;30:1222–26
11. Karagulle Kendi AT, Lehericy S, Luciana M, et al. **Altered diffusion in the frontal lobe in Parkinson disease.** *AJNR Am J Neuroradiol* 2008;29:501–05
12. Matsui H, Nishinaka K, Oda M, et al. **Dementia in Parkinson's disease: diffusion tensor imaging.** *Acta Neurol Scand* 2007;116:177–81
13. Kövari E, Gold G, Herrmann FR, et al. **Lewy body densities in the entorhinal and anterior cingulate cortex predict cognitive deficits in Parkinson's disease.** *Acta Neuropathol* 2003;106:83–88
14. Duvernoy HM. *The Human Hippocampus: Functional Anatomy, Vascularization, and Serial Sections with MRI.* Berlin, Germany: Springer-Verlag; 2005
15. Vogt BA, Nimchinsky EA, Vogt LJ, et al. **Human cingulate cortex: surface features, flat maps, and cytoarchitecture.** *J Comp Neurol* 1995;359:490–506
16. Aoki S, Iwata NK, Masutani Y, et al. **Quantitative evaluation of the pyramidal tract segmented by diffusion tensor tractography: feasibility study in patients with amyotrophic lateral sclerosis.** *Radiat Med* 2005;23:195–99
17. Kunimatsu A, Aoki S, Masutani Y, et al. **Three-dimensional white matter tractography by diffusion tensor imaging in ischaemic stroke involving the corticospinal tract.** *Neuroradiology* 2003;45:532–35
18. Hughes AJ, Daniel SE, Kilford L, et al. **Accuracy of clinical diagnosis of idiopathic Parkinson's disease: a clinico-pathological study of 100 cases.** *J Neurol Neurosurg Psychiatry* 1992;55:181–84
19. Folstein MF, Folstein SE, McHugh PR. **"Mini-mental state": a practical method for grading the cognitive state of patients for the clinician.** *J Psychiatr Res* 1975;12:189–98
20. Goetz CG, Emre M, Dubois B. **Parkinson's disease dementia: definitions, guidelines, and research perspectives in diagnosis.** *Ann Neurol* 2008;64(suppl 2):S81–92
21. Kubicki M, Westin CF, Maier SE, et al. **Uncinate fasciculus findings in schizophrenia: a magnetic resonance diffusion tensor imaging study.** *Am J Psychiatry* 2002;159:813–20
22. Pajevic S, Pierpaoli C. **Color schemes to represent the orientation of anisotropic tissues from diffusion tensor data: application to white matter fiber tract mapping in the human brain.** *Magn Reson Med* 2000;43:921
23. Mori S, Crain BJ, Chacko VP, et al. **Three-dimensional tracking of axonal projections in the brain by magnetic resonance imaging.** *Ann Neurol* 1999;45:265–69
24. Wakana S, Jiang H, Nagae-Poetscher LM, et al. **Fiber tract-based atlas of human white matter anatomy.** *Radiology* 2004;230:77–87
25. Yasmin H, Aoki S, Abe O, et al. **Tract-specific analysis of white matter pathways in healthy subjects: a pilot study using diffusion tensor MRI.** *Neuroradiology* 2009;51:831–40
26. Abe O, Aoki S, Hayashi N, et al. **Normal aging in the central nervous system: quantitative MR diffusion-tensor analysis.** *Neurobiol Aging* 2002;23:433–41
27. Firbank MJ, Blamire AM, Krishnan MS, et al. **Atrophy is associated with posterior cingulate white matter disruption in dementia with Lewy bodies and Alzheimer's disease.** *Neuroimage* 2007;36:1–7
28. Taoka T, Kin T, Nakagawa H, et al. **Diffusivity and diffusion anisotropy of cerebellar peduncles in cases of spinocerebellar degenerative disease.** *Neuroimage* 2007;37:387–93
29. Nagano-Saito A, Washimi Y, Arahata Y, et al. **Cerebral atrophy and its relation to cognitive impairment in Parkinson disease.** *Neurology* 2005;64:224–29
30. Beyer MK, Janvin CC, Larsen JP, et al. **A magnetic resonance imaging study of patients with Parkinson's disease with mild cognitive impairment and dementia using voxel-based morphometry.** *J Neurol Neurosurg Psychiatry* 2007;78:254–59
31. Camicioli RM, Korzan JR, Foster SL, et al. **Posterior cingulate metabolic changes occur in Parkinson's disease patients without dementia.** *Neurosci Lett* 2004;354:177–80
32. Vander Borght T, Minoshima S, Giordani B, et al. **Cerebral metabolic differences in Parkinson's and Alzheimer's diseases matched for dementia severity.** *J Nucl Med* 1997;38:797–802
33. Mito Y, Yoshida K, Yabe I, et al. **Brain 3D-SSP SPECT analysis in dementia with Lewy bodies, Parkinson's disease with and without dementia, and Alzheimer's disease.** *Clin Neurol Neurosurg* 2005;107:396–403
34. Mito Y, Yoshida K, Yabe I, et al. **Brain SPECT analysis by 3D-SSP and phenotype of Parkinson's disease.** *J Neurol Sci* 2006;241:67–72
35. Abe O, Yamasue H, Kasai K, et al. **Voxel-based diffusion tensor analysis reveals aberrant anterior cingulum integrity in posttraumatic stress disorder due to terrorism.** *Psychiatry Res* 2006;146:231–42
36. Buchsbaum MS, Tang CY, Peled S, et al. **MRI white matter diffusion anisotropy and PET metabolic rate in schizophrenia.** *Neuroreport* 1998;9:425–30
37. Docherty MJ, Burn DJ. **Parkinson's disease dementia.** *Curr Neurol Neurosci Rep* 2010;10:292–98
38. Mahieux F, Fenelon G, Flahault A, et al. **Neuropsychological prediction of dementia in Parkinson's disease.** *J Neurol Neurosurg Psychiatry* 1998;64:178–83
39. Brown RG, Marsden CD. **How common is dementia in Parkinson's disease?** *Lancet* 1984;2:1262–65
40. Cooper JA, Sagar HJ, Jordan N, et al. **Cognitive impairment in early, untreated Parkinson's disease and its relationship to motor disability.** *Brain* 1991;114(pt 5):2095–122
41. Lees AJ, Smith E. **Cognitive deficits in the early stages of Parkinson's disease.** *Brain* 1993;106(pt 2):257–70